The relative controls of temperature, soil moisture, and plant functional group on soil CO_2 efflux at diel, seasonal, and annual scales

Greg A. Barron-Gafford,[1,2] Russell L. Scott,[3] G. Darrel Jenerette,[4] and Travis E. Huxman[1,2]

Received 3 June 2010; revised 16 December 2010; accepted 4 January 2011; published 8 March 2011.

[1] Soil respiration (R_{soil}) is a dominant, but variable, contributor to ecosystem CO_2 efflux. Understanding how variations in major environmental drivers, like temperature and available moisture, might regulate R_{soil} has become extremely relevant. Plant functional-type diversity makes such assessments difficult because of the confounding influence of varied plant phenology and influences on soil microhabitats. We used automated measurement systems to quantify R_{soil} in the three microhabitats (under mesquites, under bunchgrasses, and in intercanopy soils) that result from mesquite encroachment into grasslands to inform our understanding of diel R_{soil} patterns in response to changes in temperature, seasonal variations in R_{soil} in response to varied soil moisture and plant phenology, and the contribution of each microhabitat to total ecosystem-scale R_{soil}. We detected a counterclockwise hysteretic response of R_{soil} to soil temperature, such that up to 100% greater fluxes were observed in the afternoon/evening than the morning for the same temperature. Phenological differences influenced ecosystem-scale R_{soil} in that mesquites were physiologically active months before bunchgrasses and R_{soil} rates under mesquites were greater and elevated longer in response to rains. Cumulative annual R_{soil} was 412, 229, and 202 g C m^{-2} under mesquites, bunchgrasses, and intercanopy spaces, respectively. Extrapolating to the ecosystem-scale using cover estimates within the site's eddy covariance footprint illustrated that average mesquite R_{soil} contributed 46% to overall ecosystem-scale R_{soil}, though mesquite composed only about 35% of the site. As grasslands transition to shrub dominance, the contribution of R_{soil} to net ecosystem flux will likely increase, potentially offsetting presumed greater CO_2 uptake potential of woody plants.

Citation: Barron-Gafford, G. A., R. L. Scott, G. D. Jenerette, and T. E. Huxman (2011), The relative controls of temperature, soil moisture, and plant functional group on soil CO_2 efflux at diel, seasonal, and annual scales, *J. Geophys. Res.*, *116*, G01023, doi:10.1029/2010JG001442.

1. Introduction

[2] A major challenge in quantifying carbon flux dynamics within the terrestrial biosphere lies in identifying whether landscapes are sources or sinks for atmospheric carbon across seasonal, annual, and decadal timescales [*Jenerette and Lal*, 2005; *Schimel et al.*, 2000; *Scott et al.*, 2009]. Because soil respiration (R_{soil}) is such a dominant contributor to total ecosystem efflux, sometimes in excess of 70% [*Law et al.*, 2001], it is important to quantify how variations in the major environmental drivers of biological activity (temperature and available moisture) might regulate R_{soil}, and thus the relative contribution of R_{soil} or changes in climate, to ecosystem source/sink status. These assessments become more difficult with increased diversity of plant functional type in a landscape because of the confounding influence of varied plant phenology, physiological responses, or the degree with which multiple growth forms differentially influence soil microhabitats.

[3] One such driver of increased landscape patchiness is the expansion of woody plants into native grasslands. Up to approximately 60 million ha are estimated to have shifted from semiarid grassland to shrubland within western North America alone over the last century [*Van Auken*, 2000]. This expansion, termed by *Goodale and Davidson* [2002] "woody encroachment," has been attributed to a variety of factors including intense livestock grazing, altered fire regimes, climate changes and atmospheric enrichment of CO_2 [*McPherson*, 1997; *Van Auken*, 2000]. Woody plant

[1] B2 Earthscience, University of Arizona, Tucson, Arizona, USA.
[2] Department of Ecology and Evolutionary Biology, University of Arizona, Tucson, Arizona, USA.
[3] Southwest Watershed Research Center, USDA-ARS, Tucson, Arizona, USA.
[4] Department of Botany and Plant Sciences, University of California, Riverside, California, USA.

0148-0227/11/2010JG001442

encroachment has an enormous potential to alter seasonal and annual carbon fluxes, particularly in arid and semiarid (dryland) systems where water is often scarce and high temperatures are abundant. Analyses have suggested that encroachment in dryland and montane ecosystems could represent a large but uncertain portion of the North American carbon sink [*Houghton et al.*, 1999; *Hurtt et al.*, 2002; *Pacala et al.*, 2007, 2001]. The greatest gap in our understanding of ecosystem-scale carbon source/sink potential comes from our limited knowledge of the contributions of respiratory (soil and vegetative) efflux to net CO_2 exchange, particularly in mixed vegetation ecosystems.

[4] Identifying how soils under grasses, woody shrubs, and within intercanopy soils differentially respond to variations in available soil moisture and fluctuations in temperature is important for modeling rates of carbon and water flux under future encroachment and predicted climate change scenarios. Our understanding of the spatial and temporal complexity of R_{soil} has been limited by the methods available to quantify R_{soil} in the field. Portable chambers have allowed researchers to quantify spatial variation in R_{soil} [*Asensio et al.*, 2007; *Han et al.*, 2007a, 2007b; *Tang and Baldocchi*, 2005] and pulse dynamics in field experiments within which precipitation events were delivered manually [*Cable et al.*, 2008; *Potts et al.*, 2006a, 2006b; *Sponseller*, 2007]. The only means of quantifying temporal variation (including diel, seasonal, or annual scales) in R_{soil} using a portable chamber is through repeated manual measurements. Because we know nonlinearities in the responses of R_{soil} to soil moisture exist, particularly as the soil dries, one has to model intermediate points between sampling periods when conducting manual measurements [*Cable et al.*, 2008]. Alternative means by which one can quantify temporal variation in R_{soil}, include the use of automated soil chambers [*Goulden and Crill*, 1997; *Irvine and Law*, 2002; *Liang et al.*, 2003, 2004; *Savage and Davidson*, 2003; *Scott et al.*, 1999] or soil CO_2 profile measurements (first described by *Hirano et al.* [2003]). Using automated systems allows for the tracking of the up regulation and gradual decline in soil respiratory activity under various microhabitats in response to multiple precipitation events throughout a season. Having a nearly continuous data record also allows for additional analysis, such as the effects of antecedent soil moisture conditions on priming of the soil for subsequent precipitation events and temporal variation in R_{soil} rates across various scales.

[5] *Tang and Baldocchi* [2005] note that because automated systems are often expensive, temporal patterns of R_{soil} are regularly simulated using continuous records of soil temperature, soil moisture or other variables [*Davidson et al.*, 1998; *Treonis et al.*, 2002; *Xu and Qi*, 2001]. However, the spatial variation in R_{soil}, both within a site and between sites, is strongly affected by gradients in biological activity or soil properties rather than these climatic variables [*Ivanov et al.*, 2010]. In addition to the influence of topography and soil texture in moderating soil moisture at multiple spatial and temporal scales [see *Teuling and Troch*, 2005], heterogeneity in vegetation coverage from woody plant encroachment has been shown to increase spatial heterogeneity of soil resources [*Reynolds et al.*, 1999; *Schlesinger et al.*, 1990], and that heterogeneity is likely a major contributor to the spatial variation in R_{soil}. Vegetative cover change alters soil properties not only by influencing patterns of solar energy entering an ecosystem [*Zou et al.*, 2007], but also by altering patterns of rooting distributions and soil chemistry [*Jackson et al.*, 2000]. *Subke et al.* [2006] identify the major sources of CO_2 in the soil as growth and maintenance respiration by roots (true root respiration), heterotrophic decomposition of carbohydrates derived from live roots, litter, and old soil organic matter (SOM), the priming of SOM decomposition by substrate input from live roots or plant litter, and weathering of soil carbonates. The dynamics of all of these components are controlled by the concomitant effects of abiotic and biotic (aboveground vegetation structure, photosynthetic activity, and plant phenological development) factors, and nearly all sources of soil CO_2 pools are directly related to the vegetative cover present.

[6] In this paper, we explored the controls of temperature, soil moisture, and vegetation cover on R_{soil} in a semiarid grassland that has been encroached by *Prosopis velutina*. Within this encroached ecosystem, now a savanna, there are three main microhabitats that may affect the magnitude and timing of R_{soil}, and it is in this context that we address the following questions: (1) What are the relative contributions of the three main microhabitats (under mesquites, under bunchgrasses, and in the intercanopy soil space) that develop as a result of woody plant encroachment to total ecosystem-scale R_{soil}? (2) What is the role of antecedent soil moisture in influencing R_{soil}, and how does that differ among these microhabitats? (3) How sensitive are rates of R_{soil} under these different microhabitats to changes in temperature, and do those sensitivities change in response to variation in soil moisture? (4) How might variation in these temperature sensitivities among microhabitats and seasons within a year differentially influence total ecosystem-scale R_{soil}?

2. Methods

2.1. Study Site Description

[7] This study was conducted within the Santa Rita Experimental Range (31.8214°N, 110.8661°W, elevation 1116 m) outside of Tucson, Arizona. An eddy covariance tower has been in place at this site since 2004, and the details of the instrumentation and processing are fully described by *Scott et al.* [2009]. Briefly, the 8 m tower logs 30 min averages of carbon dioxide and water exchange and all associated micrometeorological data, including measures of air temperature, vapor pressure deficit, pressure, incoming photosynthetically active radiation (PAR), long- and shortwave radiation and precipitation. Measures of net ecosystem exchange of carbon dioxide (NEE; μmol m^{-2} s^{-1}) were partitioned into gross ecosystem production (GEP) and ecosystem respiration (R_{eco}). Thirty minute averages of R_{eco} were estimated by fitting an exponential function to air temperature and nighttime NEE data over a moving ~5 day window after *Reichstein et al.* [2005]. Missing nighttime NEE data and daytime respiration data were also filled according to this model. A nonrectangular hyperbolic light response function based on a 15 day moving window of NEE and PAR were used to fill missing daytime NEE values

[*Gilmanov et al.*, 2007; *Scott et al.*, 2009]. Ultimately, GEP was determined according to

$$\mathrm{GEP} = R_{\mathrm{eco}} - \mathrm{NEE} \quad (1)$$

Data from the eddy covariance tower were used to compare estimates of ecosystem-scale soil respiration (detailed below) with total respiration from the aboveground and belowground portions of the ecosystem (R_{eco}) and to use GEP as a corollary for CO_2 input by way of ecosystem photosynthesis. Throughout the last century, the rangelands surrounding this site have transitioned from a semiarid grassland to a savanna by the encroachment of a woody leguminous tree [*Glendening*, 1952; *McClaran*, 2003]. Velvet mesquite (*Prosopis velutina* Woot.) now dominates this site, covering approximately 35% of a 200 m diameter area within the footprint of this tower. Much of the space between the mesquite canopies now consists of a mosaic of bunchgrasses (*Eragrostis lehmanniana* Nees, *Digitaria californica* Benth, *Muhlenbergia porteri*, and *Bouteloua eriopoda*) and seasonally bare, sandy soil (hereafter referred to as intercanopy space). Total canopy cover of perennial grasses, forbs and subshrubs at this site was approximately 22% [*Scott et al.*, 2009]. Winter and summer annuals can occupy more than half or the remaining 45% of intercanopy space in response to prolonged seasonal wetting. Mean annual precipitation at the site is 375 mm, with about 50% falling in July–September as part of the North American Monsoon.

2.2. Soil Respiration Measurements

2.2.1. Automated Instrumentation Using the Gradient Method

[8] The most common means of measuring R_{soil} by way of the "gradient method" is to use solid-state CO_2 sensors [*Baldocchi et al.*, 2006; *Myklebust et al.*, 2008; *Riveros-Iregui et al.*, 2007, 2008; *Tang et al.*, 2003, 2005a, 2005b; *Vargas and Allen*, 2008a, 2008b, 2008c]. CO_2 naturally absorbs light in certain wave bands of the infrared region of the electromagnetic spectrum, and this absorption is utilized to measure volumetric CO_2 concentration ($[CO_2]$) in compact probes (GM222, Vaisala, Helsinki, Finland; http://www.vaisala.com). *Tang et al.* [2003] provide a thorough description of the mechanics of the sensors. Briefly, the CO_2 sensor consists of three parts (a remote probe, a transmitter body, and a cable) whose function is managed by a data logger through a multiplexer (CR10X and AM16, respectively, Campbell Scientific Inc., Logan, Utah). Using a multiplexer allowed for installation of soil moisture probes (CS616, Campbell Scientific Inc., Logan, Utah) and soil temperature probes (T108, Campbell Scientific Inc., Logan, Utah) in conjunction with each CO_2 sensor. Holes on the surface of the CO_2 sensor allowed CO_2 to diffuse three dimensionally through a membrane surrounding the probe. Each probe was encased in a vertical pipe with an open bottom that terminated at the desired depth in the soil, and this casing was sealed on the upper end using a rubber gasket that fits snugly between the probe and the pipe housing. $[CO_2]$ at each depth was scanned every 30 s, and 5 min averages were stored in the data logger. The $[CO_2]$ readings were corrected for field variations in temperature and pressure using the aforementioned data collected by the eddy covariance tower [*Tang et al.*, 2003].

[9] Each enclosure box was built to control six solid-state CO_2 sensors and all accompanying soil moisture and temperature probes. Two CO_2 sensors (with a range of 0–5000 μmol mol^{-1}) were installed at depths of 2 and 10 cm. Within a separate analysis, a comparison between this setup and a three-depth (2, 8, and 16 cm) installation was made over a 6 month period, and there was no significant difference between the resulting R_{soil} estimates. Therefore, the two-probe installation was used within this study to maximize opportunity for quantification of spatial variation due to between-microhabitat differences. Soil temperature was measured at 2, 10, and 16 cm depths, and a soil moisture probe was installed to integrate across the 0–10 cm depth. This setup was deployed in January 2007 in each of three microhabitats (under mesquite, under grass [*Digitaria californica*], and in the intercanopy space).

[10] Ultimately, R_{soil} is calculated using Fick's first law of diffusion through the following series of equations:

$$F = -D_{\mathrm{s}} \frac{\mathrm{d}C}{\mathrm{d}z} \quad (2)$$

where F is CO_2 efflux from the soil (μmol m^{-2} s^{-1}), D_{s} is the CO_2 diffusion coefficient in the soil (m^2 s^{-1}), and dC/dz is the vertical soil CO_2 gradient. D_{s} can either be calculated from physical properties of the soil and soil climate or from transport tracer measurements (as described by *Davidson and Trumbore* [1995]). When calculated, as done here, the equation used is

$$D_{\mathrm{s}} = \xi D_{\mathrm{a}} \quad (3)$$

where ξ is the gas tortuosity factor and D_{a} is the CO_2 diffusion coefficient in free air. Of all the parameters involved in calculating CO_2 efflux, the ξ is among the most important and the most contentious. The ξ describes the cross-sectional area of soil available for flow and the higher diffusion resistance that exists in soil than in air [*Uchida et al.*, 1997]. Several empirical models for computing ξ have been developed in the lab and examined in the field [*Hillel*, 1993; *Jury et al.*, 1991]. *Moldrup et al.* [1999] have generated a calculation of ξ using a model based on diffusion through a porous media that has become widely adopted [*Baldocchi et al.*, 2006; *Turcu et al.*, 2005; *Vargas and Allen*, 2008b]:

$$\xi = \phi^2 \left(\frac{\alpha}{\phi}\right)^{\beta S} \quad (4)$$

where α is volumetric air content (air-filled porosity), ϕ is soil porosity, β is a constant (2.9), and S (unitless) = silt + sand content. In both equations, ϕ is calculated using measures of volumetric water content, bulk density, and particle density for the mineral soil. The Moldrup equation was used in the present study because of the better fit between measurement techniques it yielded within this and the aforementioned studies and the goodness of fit others have found between measured and modeled estimates of R_{soil} [*Suwa et al.*, 2004].

[11] The vertical gradient of soil $[CO_2]$ and a gaseous diffusion coefficient of soil CO_2 are substituted into the

diffusion equation of Fick's law, as described in equation (2) [*Hirano et al.*, 2003; *Tang et al.*, 2003; *Vargas and Allen*, 2008b]. Through a linear regression of [CO_2] over a depth, a slope is computed and used to represent the [CO_2] gradient. Soil [CO_2] have been shown to increase linearly with depth until reaching a certain, deep level where it either becomes constant if a barrier is present or decreases if there is no barrier [*Baldocchi et al.*, 2006; *Jury et al.*, 1991], however such an assumption should be examined at each study site. A linear extrapolation to estimate CO_2 flux at the surface (R_{soil}) is used based on this assumption that CO_2 production is constant in the soil profile.

[12] Similar to *Riveros-Iregui et al.* [2007], we calculated a daily measure of the degree of hysteresis in the relationship between soil temperature and R_{soil}. The degree of hysteresis was quantified as the difference between maximum and minimum rate of R_{soil} for the median temperature within the range each microhabitat experienced within a 24 h period. In this way, we developed a microhabitat-specific measure of the difference between midmorning and evening R_{soil} [μmol CO_2 m^{-2} s^{-1}] for a common soil temperature.

2.2.2. Manual Measurements

[13] R_{soil} was also measured using manual instruments and permanently installed soil collars. Soil collars, each with a diameter of 10.2 cm, were installed to a depth of 5 cm within each of the three microhabitats every 10 m along two 50 m transects. Transects ran west and south from the eddy covariance tower, for a total of 15 collars per transect. At each 10 m interval point, the location and cardinal position of each microhabitat collar were randomly determined. Sample collars were located in the middle of the vertically projected crown radii for the vegetated microhabitats. Two additional soil collars were installed in conjunction with each of the aforementioned automated measurement systems so that direct comparisons of measurement systems could be made. R_{soil} was measured using a custom 3 L soil chamber connected to a portable CO_2 gas analyzer (LI-820, LI-COR Biosciences, Nebraska) interfaced with a laptop for data collection and storage, as described by *Cable et al.* [2008]. At each collar, soil moisture integrated over a 12 cm depth was measured using a handheld water content sensor (HydroSense system, CSI), and soil temperature across 10 cm was measured using a temperature probe (Temp-100, OAKTON Instruments, Illinois). R_{soil} at each collar was measured at least once every two weeks along the full transect and in the paired collars. In order to capture the full suite of soil conditions, biweekly measurement were sometimes supplemented to capture measures of R_{soil} immediately before and the day of rain events.

2.3. Extrapolating to the Ecosystem Scale and Statistical Analysis

[14] In order to upscale our estimates of soil respiration within the three microhabitats to the ecosystem scale, we used a simple scaling model

$$\text{Ecosystem-scale } R_{soil} = F_{mesquite} \times R_{mesquite} + F_{grass} \times R_{grass} + F_{intercanopy} \times R_{intercanopy} \quad (5)$$

where F is the fraction of cover at the site and R is rates of soil respiration for that microhabitat for that 30 min period. The contribution of each microhabitat to this total ecosystem-scale R_{soil} was calculated individually for each 30 min timestamp by

$$(F_{microhabitat}/R_{microhabitat})/\text{Ecosystem-scale } R_{soil} \quad (6)$$

[15] The relationships between chamber-based measurements and gradient method estimates of R_{soil} for each microhabitat were calculated using a Spearman's correlation analysis to generate r^2 values. We then used a geometric mean/reduced major axis regression analysis as described by *Ricker* [1973] to account for uncertainties in both the chamber and gradient method measures of R_{soil} for each microhabitat. These analyses were performed in MATLAB 2009b (MathWorks, Natick, Massachusetts) using a user-community-generated program, the code for which can be accessed online (A. Trujillo-Ortiz and R. Hernandez-Walls, gmregress: Geometric Mean Regression (Reduced Major Axis Regression), A MATLAB file, 2010, available at http://www.mathworks.com/matlabcentral/fileexchange/27918-gmregress). Kruskal-Wallis one-way analyses of variance were used to test for differences in means of R_{soil} rates between the three microhabitats (under mesquite versus under grass versus in intercanopy soil space), the six seasonal periods, prerain and postrain events. The Kruskal-Wallis one-way analysis of variance is a nonparametric method for testing the equality of groups of data, such that differences in means among multiple groups or within a single group among different time periods can be measured against the null hypothesis that there is no difference among sample means. One-way repeated measures ANOVA (Holm-Sidak method) t tests for multiple comparisons were made using MATLAB 2009b to compare R_{soil} rates among seasonal periods for each microhabitat.

3. Results

[16] R_{soil} was monitored throughout 2007 in order to quantify rates of R_{soil} under these different microhabitats and their responses to changes in temperature and variations in near-surface soil moisture. The yearlong study was broken into six seasonal periods based on characteristic temperature, precipitation, and soil moisture conditions. The *late winter* months (DOY 0–85) were cool, but the soil became progressively drier and warmer as cool season rains faded. During the *premonsoon* period (DOY 86–189) the site became increasingly hot, with daytime maximum air temperatures exceeding 35°C and soil temperatures approaching 50°C near the end. This period was characterized as having little rainfall; however, the site experienced two isolated precipitation events. Rains associated with the North American monsoon started on DOY 189 and ended on DOY 271. We separated this period into two blocks (*early* and *late monsoon*) to better understand the effects of phenology. The *postmonsoon* period (DOY 272–335) was characterized by progressively drier conditions and cooling temperatures, and by the *early winter* (DOY 336–365) the site experienced occasional nighttime frosts and cool season rains.

3.1. Measurement Comparisons and Validation of the Gradient Method

[17] Estimates of R_{soil} from the chamber method and gradient method showed a significant positive relationship

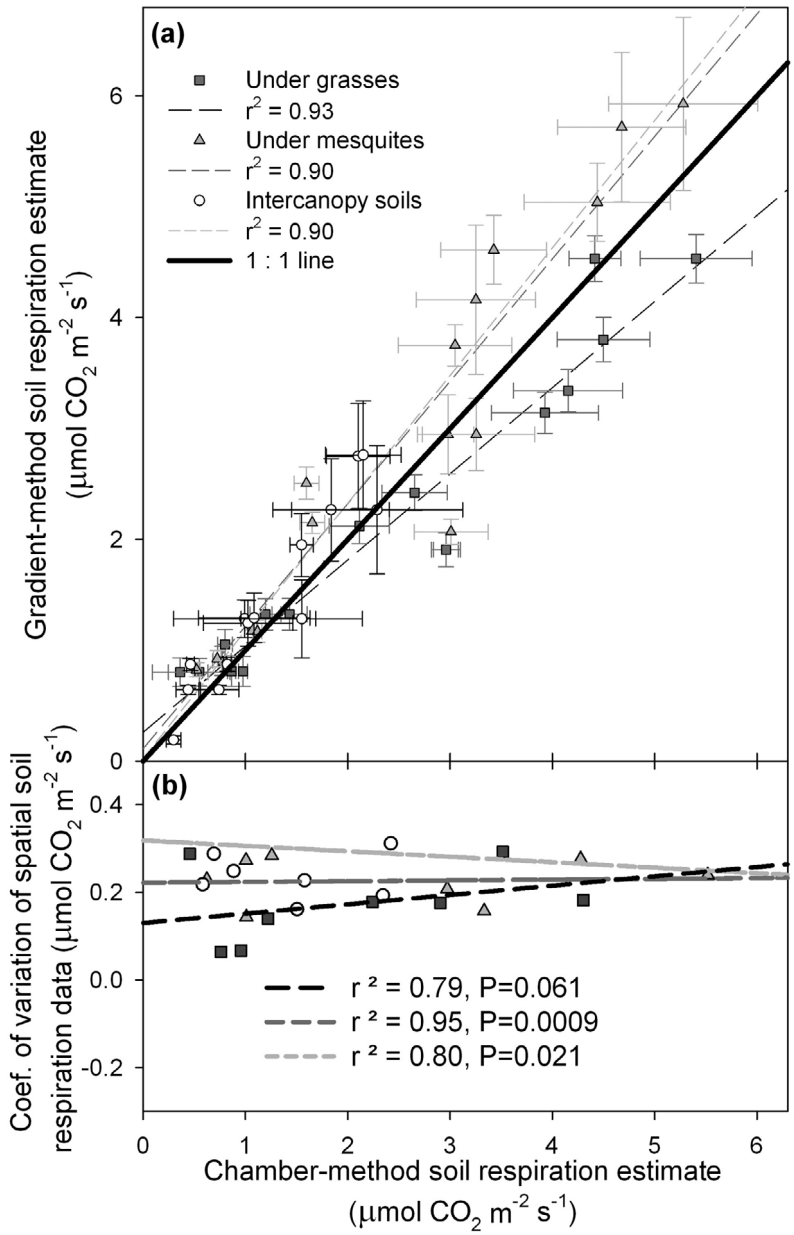

Figure 1. (a) Comparison among manual chamber soil respiration measurements and those obtained simultaneously by the automated, gradient method illustrate a significant positive relationship between the techniques throughout the year within each of the microhabitats and no significant difference from the 1:1 line. Vertical error bars correspond to error associated with the spatially extensive manual soil respiration measurements, and horizontal error bars relate to the temporally intensive gradient method measurement. (b) The coefficient of variation of the manual soil respiration data collected throughout the year relative to the magnitude of soil respiration rates within each microhabitat.

between the techniques throughout the year within each of the microhabitats (Figure 1a). We detected a significant positive correlation ($P < 0.0001$ for all microhabitats) between the two methods for measures under the bunchgrasses ($r^2 = 0.93$), under mesquites ($r^2 = 0.90$) and in the intercanopy spaces ($r^2 = 0.90$). The intercepts were not significantly different from zero, and the slopes were not significantly different from the 1:1 line for any microhabitats. There was no significant trend in the coefficient of variation (standard deviation divided the mean) for the spatially distributed R_{soil} (Figure 1b). As noted above, soil CO_2 concentrations from two depths were used in this gradient method installation, and CO_2 concentration was assumed to have increased linearly with depth. The validity of this assumption was tested in a separate analysis of soil CO_2 concentrations among three depths used in a temporary three-probe installation. Though the range of the standard errors overlap between the two deeper depths, plots of relative CO_2 concentration (normalized for each seasonal bin) against depth below the soil surface demonstrate a

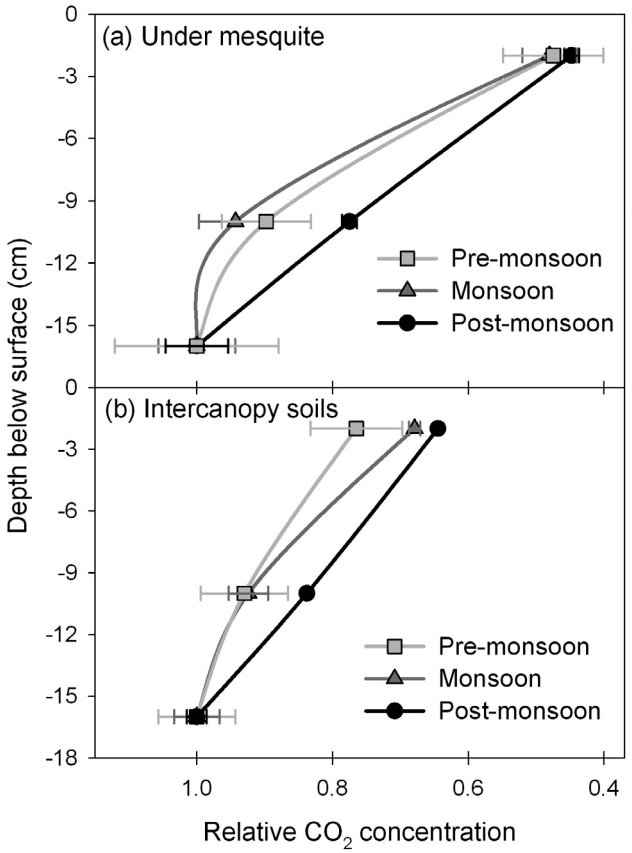

Figure 2. Seasonal averages of relative soil CO_2 concentrations for subsurface soil depth. Each seasonal bin illustrates a 20 day average of soil CO_2 concentrations normalized to their maximum within that bin, allowing for comparisons of the linearity of CO_2 concentrations with depth among seasonal periods in which absolute concentrations differed dramatically. Results are shown for the (a) mesquite and (b) intercanopy soils where CO_2 concentrations at three depths were logged in a separate analysis. Error bars in all plots represent plus/minus one standard error of the mean.

nonlinearity in soil CO_2 concentrations at depth, particularly for soils under mesquites (Figure 2a). This trend would suggest that estimates of soil respiratory fluxes under mesquite could be somewhat overestimated, which corresponds with a slight positive bias detected between the gradient and chamber-based methods for soil efflux under mesquite. A similar, though more muted, potential nonlinearity was also detected within intercanopy soils (Figure 2b), which correlates with a smaller positive bias among the methodologies. Having conducted parallel chamber-based measures of R_{soil} across the entire suite of environmental conditions experienced by this system, we know that this nonlinearity was not substantial enough to have led to a significant misestimation of R_{soil} (Figure 1a), highlighting the need for concomitant measures when using this gradient method. Taken together, these data gave us confidence in using the results of the two methods interchangeably when quantifying interpatch differences and extrapolating to estimates of ecosystem-scale respiratory efflux.

3.2. Microhabitat Environmental Conditions

[18] Average 0–10 cm soil temperatures peaked in the premonsoon period, approaching 50°C in the early afternoon (Figure 3a). Differences among the microhabitats were made in reference to those found under the bunchgrasses, as these were the native vegetative communities prior to woody plant encroachment. Particularly during the premonsoon, daytime soil temperatures were sometimes nearly 10°C hotter in the intercanopy spaces than under bunchgrasses; the shade of the mesquite, however, kept surface temperatures significantly cooler during the day (Figure 3b). Average 0–10 cm volumetric water content (VWC) ranged from approximately 2.5% during dry periods to nearly 10% during the rainy periods (Figure 3c). With the exception of the winter periods, intercanopy soils were drier than the soils under the bunchgrasses, though intercanopy soils were occasionally the wettest microhabitat immediately after rain events. The shallow depth soils under the mesquites were consistently wetter than areas under the grasses, and the differences in soil moisture between mesquites and grasses were less variable than the differences between the grasses and intercanopy soils (Figure 3d).

3.3. Soil Respiration Under the Microhabitats Throughout an Annual Cycle

[19] Soil respiration rates differed among the microhabitats throughout the year in response to seasonal changes in soil temperature and variations in soil moisture (Figure 3e). Average R_{soil} rates during the nonmonsoonal periods were 0.4, 0.8, and 0.4 μmol CO_2 m^{-2} s^{-1} under the bunchgrasses, mesquites, and intercanopy spaces, respectively, illustrating that R_{soil} fluxes were over 111% greater under mesquites than under grasses throughout these periods ($H_{df=2}$ = 162.976; $p < 0.001$). Average daily maxima were largely responsible for differences in daily averages, as there were little differences among daily minima. During the monsoon, R_{soil} fluxes averaged 2.2, 3.9, and 1.8 μmol CO_2 m^{-2} s^{-1} under the grasses, mesquites, and intercanopy spaces, respectively, indicating a 459% ($F_{df=1}$ = 1498.5; $p < 0.001$), 361% ($F_{df=1}$ = 721.5; $p < 0.001$), and 362% ($H_{df=1}$ = 1206.5; $p < 0.001$) increase during the monsoon season over nonmonsoon flux rates, respectively. The greatest percentage of increase with the onset of the monsoon, therefore, occurred under the grasses.

[20] In order to quantify the effects of temperature and soil moisture on R_{soil} in the different microhabitats, the yearlong data set was broken into the six different seasonal periods described above (Figure 4). Regardless of season, R_{soil} under the mesquites had a daily minimum that was shifted toward later in the morning and a peak that occurred later in the afternoon, relative to the other microsites. During the late winter, average R_{soil} was relatively low; however, there were still significant differences in rates among the microhabitats (Figure 4a; under mesquites $\gg$ under grasses $\gg$ intercanopy soils; $H_{df=2}$ = 2339.43; $p < 0.001$). VWC of the soil averaged 5.0%, and air temperature, soil temperature, and vapor pressure deficit (VPD) remained relatively low throughout this period. During the dry premonsoon, all but midday R_{soil} rates were slightly greater in the intercanopy soil space than under the grasses, though R_{soil} under

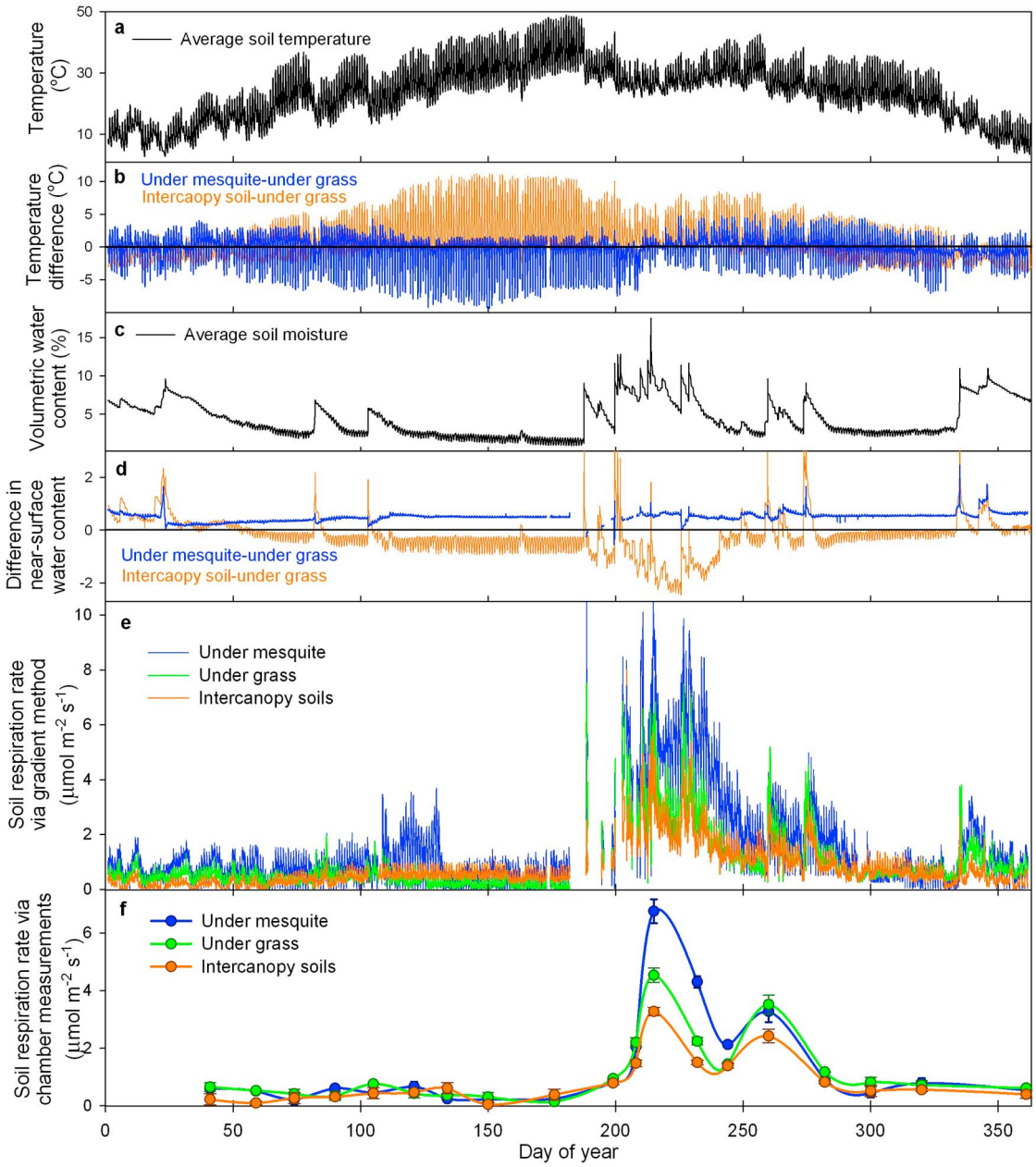

Figure 3. (a) Average 0–10 cm soil temperature under all microhabitats and (b) the difference in average soil temperatures under mesquite and in intercanopy soil space, relative to the soil under grass. Differences among microhabitats were given relative to those under grasses, the native vegetation in the ecosystem, to indicate the change from this native state. (c) Average 0–10 cm soil moisture under all microhabitats and (d) the difference in soil moisture under mesquite and in the intercanopy soil space, relative to the soil under grass. (e) Thirty minute averages of soil respiration rates, as estimated by the gradient method, for each microhabitat. (f) Daily averages of spatially extensive soil respiration measures made using a portable chamber.

the mesquites were significantly greater than both grass and intercanopy microhabitats (Figure 4b; $H_{df=2} = 3022.7$; $p < 0.001$). VWC dropped to an average of 2.6%, and average surface soil temperature and maximum incoming photosynthetically active radiation (PAR) were all greatest during this premonsoon period. Throughout the premonsoon, intercanopy soils warmed quickest and reached the highest temperatures with an average maximum 40.4, versus 37.3 and 35.1°C under the grasses and mesquites, respectively (Figure 4b, bottom). R_{soil} was greatest throughout the wet early monsoon, with R_{soil} averaging 3.2, 5.4, and 2.5 μmol CO_2 m^{-2} s^{-1} under the grasses, mesquites, and intercanopy spaces, respectively (Figure 4c). VWC climbed to an average of 7.5%, peaking at 17.5%, and there was less diel variation in soil temperature under all microhabitats, as nighttime minima were greatest during this period. R_{soil} rates

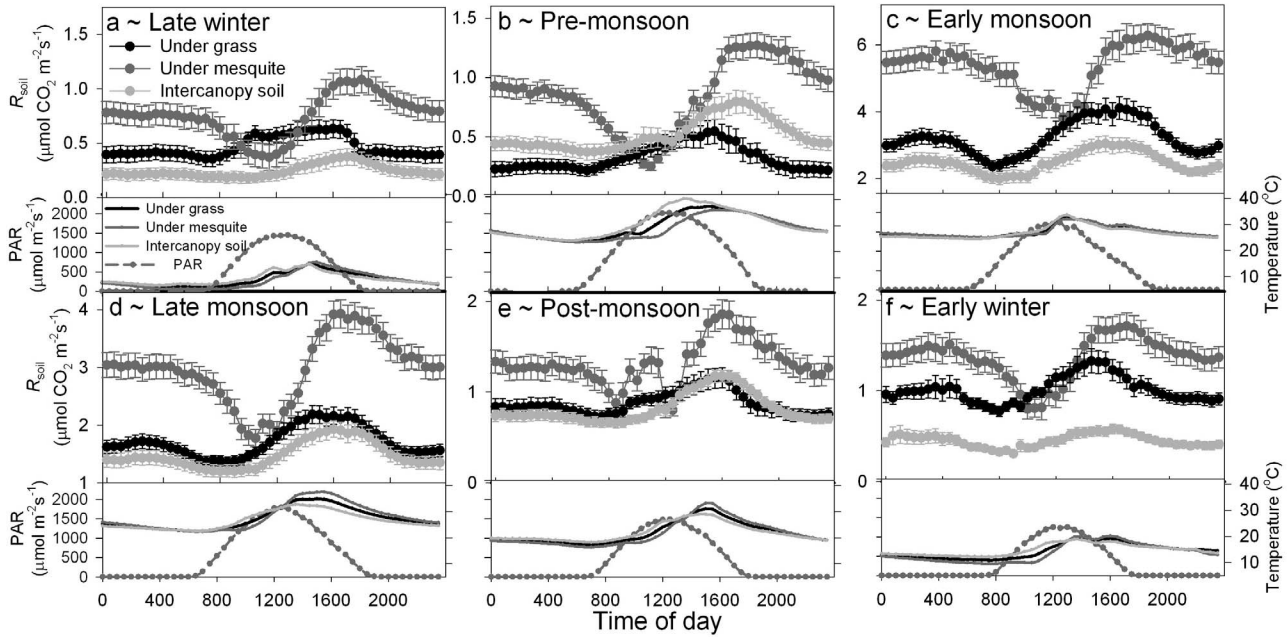

Figure 4. Average diel soil respiration (R_{soil}) and 0–10 cm soil temperature within each microhabitat and above canopy, incoming photosynthetically active radiation (PAR), throughout each of six seasonal periods consisting of late winter (DOY 0–85), premonsoon (DOY 86–189), early monsoon (DOY 190–230), late monsoon (DOY 231–271), postmonsoon (DOY 272–335), and the early winter (DOY 336–365). Error bars in all plots represent plus/minus one standard error of the mean.

dropped in all microhabitats by the late monsoon, though on average, R_{soil} under the mesquites remained approximately 73% greater than under the grasses (Figure 4d; $H_{df=1}$ = 959.3; $p < 0.001$). As average soil moisture declined during the postmonsoonal period to an average of 3.2%, so did R_{soil} rates in all microhabitats (Figure 4e). Average R_{soil} throughout this 60 day period remained significantly greater under the mesquites than the grasses ($H_{df=1} = 193.2$; $p < 0.001$).

3.4. Soil Respiration Responses to Precipitation Events: The Role of Antecedent Soil Moisture and Phenology due to Vegetative Cover

[21] Data associated with single precipitation events in the dry premonsoon (DOY 104; Figures 5a–5c) and wet monsoon (DOY 213; Figures 5d–5f) were isolated from the data set to illustrate the role of antecedent soil moisture conditions on R_{soil} rates under each of the microhabitats. Selected

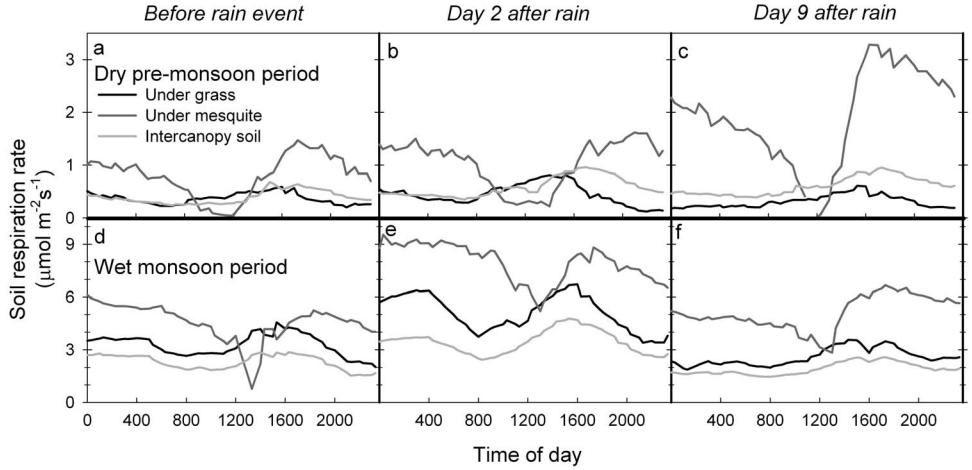

Figure 5. A closer examination of (a–c) an isolated rain event that occurred within the dry premonsoon and (d–f) an event that occurred within the wet monsoon. Thirty minute averages of soil respiration are given the day prior to the rain event, 2 days after the rain, and an additional week later (9 days after the precipitation event).

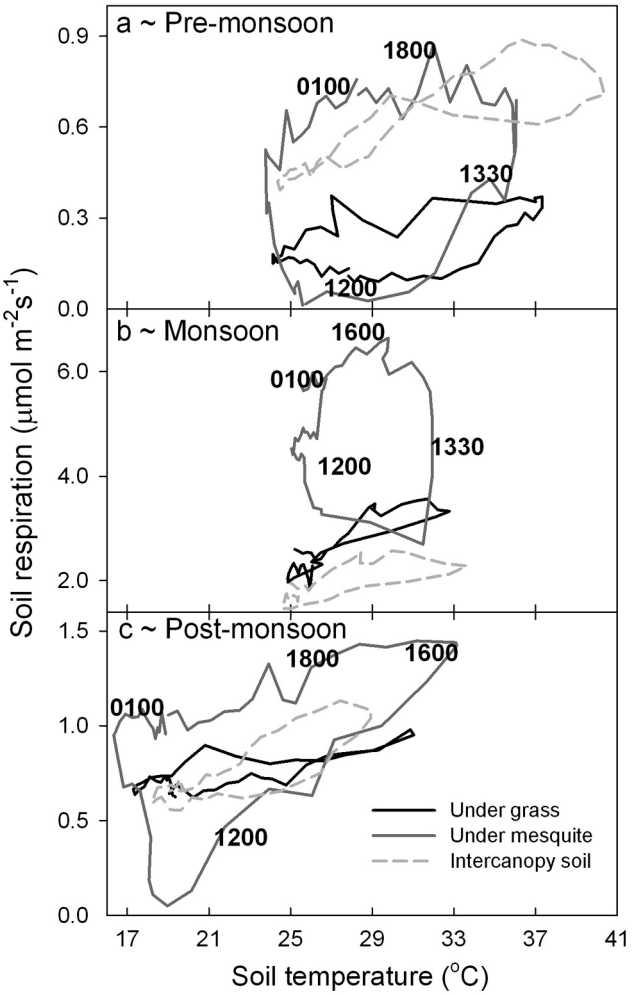

Figure 6. Average diel soil respiration rates plotted against average soil temperatures within each microhabitat, revealing a significant counterclockwise hysteretic relationship. Though the counterclockwise hysteresis occurred throughout the year, it was greatest in the (a) premonsoon, (b) monsoon, and (c) postmonsoon periods.

events occurred more than 5 days after another rain event, based on previous work suggesting that biological pulses are stimulated for up to 5 days following a precipitation event [*Jenerette et al.*, 2008], and were not followed by another measureable rain for 9 days, allowing for an analysis of the longer-term effects on R_{soil}. As noted above, R_{soil} during the dry premonsoon were relatively low, averaging 0.4, 1.0, and 0.4 μmol CO_2 m^{-2} s^{-1} under the grasses, mesquites, and intercanopy spaces, respectively (Figure 5a). Two days after the rain event, average R_{soil} rates increased approximately 11, 25, and 16% under these same microhabitats. After an additional week (9 total days after the rain event) R_{soil} had returned to preevent rates under the grasses and remained slightly elevated in the intercanopy soils. Under mesquites, however, R_{soil} rates had doubled over preevent efflux levels and were averaging more than 90% greater than efflux rates under the grasses (Figures 5a and 5c; $H_{df=1} = 55.935$; $p < 0.001$).

[22] In contrast to the premonsoon data, R_{soil} rates were already elevated prior to the isolated monsoon event, averaging 3.3, 4.5, and 2.3 μmol CO_2 m^{-2} s^{-1} under the grasses, mesquites, and intercanopy spaces, respectively (Figure 5d). Two days after a rain event, R_{soil} was elevated by more than one third in all microhabitats over preevent flux rates. However, a week later after soil moisture had decreased, daily cumulative R_{soil} under the grasses and in the intercanopy soils were 20 to 25% lower than preevent rates ($H_{df=1}$ = 26.693 and 20.215, respectively; $p < 0.001$). Conversely, R_{soil} under the mesquite remained elevated ($H_{df=1} = 5.094$; $p = 0.024$), indicating that the influence of a single rain event persisted at least 9 days under the mesquite but not the other microhabitats. Average soil temperatures were not significantly different between these isolated premonsoon and monsoonal events or during the two periods of analysis following the rains.

3.5. Soil Respiration Responses to Temperature: Diel Variation and Hysteresis

[23] Throughout all seasons, R_{soil} under mesquites was decoupled from soil temperature, and we observed a significant hysteresis effect. The degree of hysteresis in the relationship between soil temperature and R_{soil} was quantified as the difference between maximum and minimum R_{soil} for the median temperature within the range each microhabitat experienced within a 24 h period. The hysteresis always occurred counterclockwise, with maximum rates of R_{soil} in the evening as soil temperatures were decreasing. For example, average R_{soil} rates under mesquites in the premonsoon were minimal in the morning but were 3 orders of magnitude greater in the evening when soil temperatures cooled down to the same daily median temperature (Figure 6a). The absolute magnitude of the hysteresis effect, however, was greatest throughout the monsoon (Figure 6b). During the monsoon, late morning R_{soil} rates under mesquites averaged 3.1 μmol CO_2 m^{-2} s^{-1}, at 28°C, while R_{soil} averaged 6.4 μmol CO_2 m^{-2} s^{-1} when the soil had cooled back down to 28°C around 1845 LT. This difference represents a doubling in efflux rates for a common median temperature. There was little diel variation in R_{soil} in response to temperature within the grass microhabitat and within intercanopy soils during the monsoonal periods, though this is when the greatest hysteretic effect occurred under mesquites.

[24] Plotting differences in daily R_{soil} rates due to the hysteresis effect throughout the entire study period along with soil moisture levels and precipitation events illustrates the relationship between patterns of hysteresis in relation to moisture additions to the soils (Figure 7). Precipitation events during late winter induced some hysteresis in R_{soil} under mesquites, but little under grasses or the intercanopy soils. Significant, yet transient, inductions of hysteresis can be seen in the R_{soil} rates under grasses and in the intercanopy soils throughout the monsoonal seasons and in the early winter after cool season rains dramatically wet the soils. A significantly positive relationship between the amount of hysteresis in R_{soil} rates and maximum R_{soil} rates that day was detected within each microhabitat (Figure 7, inset; $p < 0.001$ for each microhabitat). The slopes of the linear regression lines were similar for the grass and intercanopy soil micro-

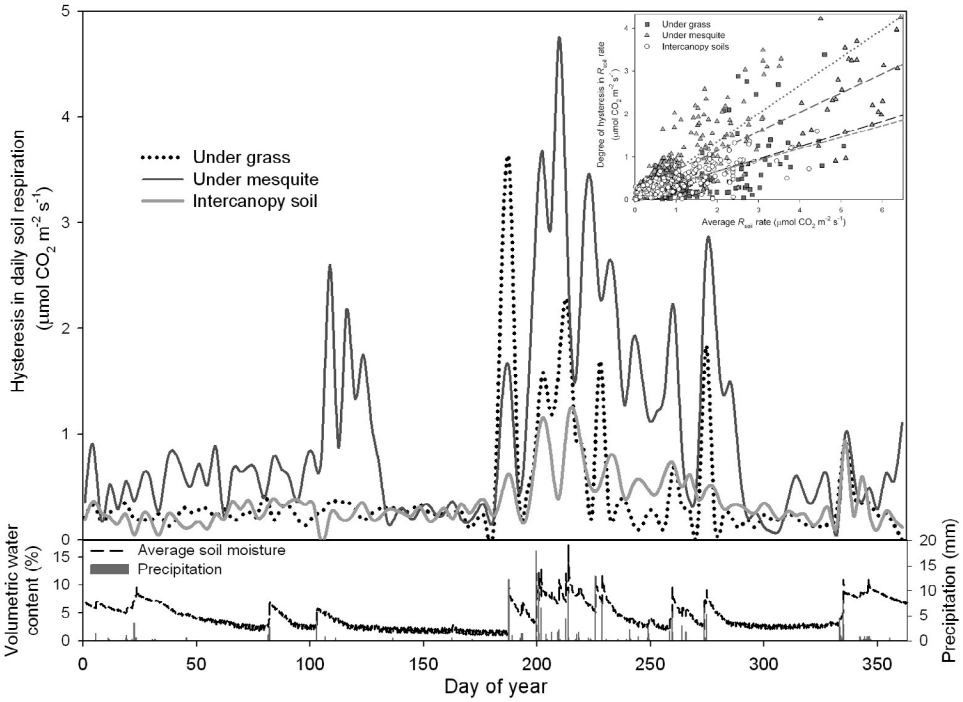

Figure 7. (top) Five day averages of the degree of hysteresis in the relationship between soil temperature and soil respiration, quantified as the difference between maximum and minimum soil respiration for the median temperature within each microhabitat within a 24 h period. Top inset shows daily maxima of R_{soil} within each of the microhabitats regressed against the degree of hysteresis in daily R_{soil} for soil under grasses (black dash), under mesquites (dark gray dash), and in intercanopy spaces (light gray, short dash). Mesquite microhabitat data from days immediately after rain events are highlighted (broader bordered triangles), and removal of these data resulted in a higher correlation and slope of the regression line. (bottom) Average soil moisture across all microhabitats and daily cumulative rain events throughout the year.

habitats (0.29 and 0.26, respectively; $p < 0.001$), but were significantly lower than that of the mesquite microhabitat (0.45; $p < 0.001$). Separating out data from the days of rain events (broader bordered triangles) from this regression for mesquites microhabitat caused a significant increase in not only the strength ($r2 = 0.40$ versus 0.62) but also the slope of the linear relationship between maximum rates of R_{soil} and degree of hysteresis in R_{soil} rates (0.45 versus 0.75; $p < 0.001$).

3.6. Contribution of Various Microhabitats to Total Ecosystem-Scale R_{soil}

[25] The contribution of each microhabitat to overall ecosystem-scale R_{soil} varied dramatically throughout the year (Figure 8a). The contribution of the mesquite and grass microhabitats was at its minimum during the premonsoon, though the contribution of the mesquite microhabitat to overall soil efflux began increasing nearly 50 days (DOY 135 versus DOY 183) before the soils under the native bunchgrasses. Averaged across the year, R_{soil} under mesquites contributed 46% ± 11 to overall ecosystem-scale R_{soil}, though mesquite vegetative cover was only about 35% at the site. Grass and intercanopy microhabitats contributed an average of 23% and 31%, respectively, to ecosystem-scale R_{soil}, and these two microhabitats composed approximately 22% and 45% of the ecosystem's cover. Thus, the average contribution of R_{soil} rates under grasses to ecosystem-scale R_{soil} was roughly equal to their percent cover, while the soils under mesquites contributed well beyond their percent coverage. The replacement of grasses at the site with mesquite and seasonally bare, intercanopy soils, therefore, resulted in greater CO_2 efflux per unit area in this semiarid ecosystem across an annual cycle. Cumulative R_{soil} for the year was 229, 412, and 202 g C m^{-2} under grasses, mesquites, and intercanopy spaces, respectively. Hence, cumulative R_{soil} was 80% greater under mesquites, and only about 11% lower in the intercanopy soil space, than under the grasses.

[26] Throughout the late winter and premonsoon, estimates of total aboveground and belowground ecosystem-scale respiration (R_{eco}) from the site's eddy covariance tower were similar to upscaled estimates of ecosystem-scale R_{soil} based on continuous measurements of CO_2 efflux and vegetative cover within the tower footprint (Figure 8b). These findings are consistent with the fact that R_{eco} is composed of aboveground and belowground pools of efflux and these periods are associated with minimal aboveground activity. Ecosystem-scale R_{soil} peaked in response to monsoon rains that began on DOY 180. Rates then dropped dramatically over the course of the next week, before rebounding throughout the monsoon. Contrary to expectations, estimates of R_{eco} were consistently less than ecosystem-scale

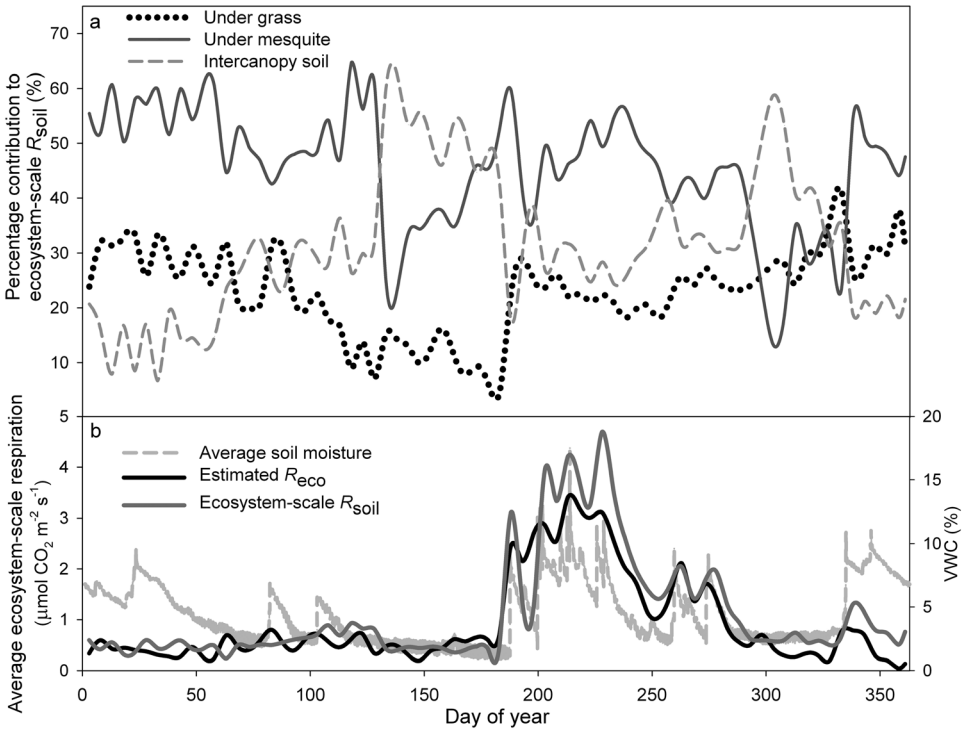

Figure 8. (a) The contribution of each microhabitat to total ecosystem-scale R_{soil} throughout the entire year based on measures of component effluxes and fraction of vegetative cover of each microhabitat within a 200 m diameter area of the footprint of the site's eddy covariance tower. (b) Five day averaged estimates of ecosystem-scale respiration from the site's eddy covariance system (R_{eco}) and extrapolated total ecosystem-scale R_{soil} throughout the year. Daily averages of average ecosystem soil moisture are also shown to illustrate CO_2 efflux rates in response to precipitation events and prolonged soil wetting.

R_{soil} from approximately DOY 200 throughout the monsoon's end when rates of both efflux parameters declined.

4. Discussion

[27] Using an automated measurement system to continuously estimate R_{soil} rates under multiple microhabitats yielded a greater understanding of the variability in R_{soil} and its relationship with soil moisture and temperature throughout an entire year for a semiarid savanna. R_{soil} rates were clearly limited by soil moisture, in that pulses of R_{soil} activity are apparent only after rain events. However, within these periods of greater available soil moisture, temperature played an important role in regulating flux rates, depending on the season and the microhabitat's dominant growth form. For example, a similar sized precipitation event induced very different rates of R_{soil} depending on whether it occurred in the hot and dry premonsoon, the wet monsoonal summer, or cooler and wet winter, likely related to both temperature-induced responses of soil microbes and aboveground vegetative responses to the rains. These dynamic relationships between rates of CO_2 efflux, abiotic drivers such as temperature and moisture, and phenological variations due to differences in microhabitat demonstrate the complexity in estimating respiratory CO_2 efflux in mixed vegetation ecosystems.

4.1. The Relative Contributions of the Three Main Microhabitats to Ecosystem-Scale R_{soil}

[28] Increases in plant growth form diversity have been shown to influence hydrologic processes due to increased variation in traits such as vertical root distribution [*Schenk and Jackson*, 2002] and maximum rooting depth [*Canadell et al.*, 1996]. As woody plants, in particular, move into grasslands, they can alter ecosystem water balance by furthering the depth from which plants extract water for transpiration [*Hultine et al.*, 2006]. Additionally, woody plants influence ecohydrological dynamics by physically altering microscale energy balance through increased attenuation of incoming solar radiation [*Martens et al.*, 2000; *Villegas et al.*, 2010a, 2010b], which, as shown here, induced cooler surface soil temperatures [*McLain et al.*, 2008; *Villegas et al.*, 2010b] and lessened evaporative potentials [*Breshears et al.*, 2009; *Scholes and Archer*, 1997; *Stark*, 1994; *Villegas et al.*, 2010a, 2010b]. Taken together, modulated soil temperatures and greater available surface soil water interacted to drive increased biological activity.

[29] Within this study, average R_{soil} rates were significantly greater under mesquites than under grasses for nearly 30 days during the premonsoon following a single isolated rain event, but only after the aboveground portion of the mesquites became physiologically active. R_{soil} rates increased more rapidly and remained higher longer after this pre-

monsoon rain in the intercanopy soils than under the grasses, likely due to the breakdown of labile soil organic matter from the abundant pool of ephemeral plants that emerged in the late winter. Grasses have fewer resources allocated toward root biomass than woody plants, and this constrained their phenology throughout the premonsoon and during the transition to the early monsoon period because they must generate the necessary absorptive roots. Additionally, mesquite deposition of abundant and easily decomposable, N-rich litter has been shown to increase soil CO_2 concentrations [*McLain et al.*, 2008], subcanopy soil organic carbon and total nitrogen [*Hibbard et al.*, 2001; *McCulley et al.*, 2004; *Throop and Archer*, 2008], and ultimately greater ecosystem-scale respiration within woodlands [*Scott et al.*, 2006].

[30] Soils under mesquites contributed significantly more to ecosystem-scale R_{soil} than any other microhabitat because of the concomitant results of (1) greater average baseline rates of R_{soil} under mesquites, (2) a more prolonged period of efflux in response to rains, and (3) the phenologically based extension of the mesquite growing season, and therefore lengthened period of R_{soil}. Cumulative R_{soil} under mesquites was ultimately 63% greater than that under grasses by the end of the year; similar significantly greater cumulative fluxes below mesquite canopies have been found using extrapolations from noncontinuous, manual measurements [*McCulley et al.*, 2004; *McLain and Martens*, 2006; *McLain et al.*, 2008]. As such, the conversion of semiarid grasslands to mixed shrublands and woodlands is likely to yield a significantly greater respiratory loss of CO_2 from the soil.

4.2. The Role of Antecedent Soil Moisture in Influencing R_{soil} and Variation in Responses Among Microhabitats

[31] Predictions as to how the monsoon rainfall might change remain uncertain [*Lin et al.*, 2008], but one consistent projection is greater interannual variability in the size and distribution of summer rains [*Diffenbaugh et al.*, 2008; *Easterling et al.*, 2000; *Gordon et al.*, 1992; *Groisman et al.*, 1999]. An important interaction between antecedent soil moisture conditions and vegetative cover type was illustrated within this study. R_{soil} rates under mesquites were elevated for more than a week after a single rain event when antecedent conditions were very dry, while R_{soil} under grasses increased only slightly and for a short period of time. These differences were likely due to contrasts in vegetative productivity between the growth forms at this stage in the year. When mesquites had not fully expanded their canopies at the onset of this rain, there was a less significant response; it was only after leaf-out that R_{soil} was stimulated. During the rainy season when both growth forms were physiologically active and a rain event came after a 5 day dry period, R_{soil} under grasses and in intercanopy soils peaked within a few days before dropping 25% below preevent rates. R_{soil} under mesquites, however, peaked within a few days and then returned to preevent rates, suggesting a more ephemeral pool of carbon stores in the other microhabitats and illustrating a sustained effect of precipitation on R_{soil} under mesquites. Such amplified responses of R_{soil} to precipitation under dry antecedent conditions relative to wetter conditions have been shown before [*Cable et al.*, 2008], though the variation between life-forms was not previously highlighted. Extrapolating these patch-scale responses to entire ecosystems, similar sporadic precipitation patterns would result in very different carbon balances depending on the vegetative composition of the ecosystem. Grasslands will likely have small and transient responses of R_{soil} to such precipitation patterns. In contrast, mixed vegetation shrublands and woodlands are liable to efflux more CO_2 to the atmosphere by way of R_{soil} and for longer periods after each rain. These results underscore both the need for continuous measurement systems to capture these important findings and the necessity of examining multiple components within a mixed vegetation system.

4.3. The Sensitivity of R_{soil} Rates Under These Different Microhabitats to Changes in Temperature and the Concomitant Influence of Varied Available Soil Moisture

[32] Continuous estimation of R_{soil} throughout diel periods elucidated important trends in the response of R_{soil} to changes in soil temperature. Rather than finding a simple Arrhenius [*Lloyd and Taylor*, 1994] or Q_{10} [*Raich and Schlesinger*, 1992] relationship between increasing soil temperatures and R_{soil}, we found a seasonally significant hysteresis effect that itself did not follow an Arrhenius or Q_{10} function, similar to that shown by *Riveros-Iregui et al.* [2007]. Recently, an increasing number of studies using automated R_{soil} measurement systems have shown a diel hysteresis in the relationship between R_{soil} and soil temperature [*Carbone et al.*, 2008; *Gaumont-Guay et al.*, 2006; *Parkin and Kaspar*, 2003; *Riveros-Iregui et al.*, 2008; *Ruehr et al.*, 2010; *Tang et al.*, 2005a; *Vargas and Allen*, 2008b, 2008c]. Within this study, as in the studies by *Tang et al.* [2005a] and *Gaumont-Guay et al.* [2006], the hysteresis effect occurred counterclockwise (Figure 6), such that higher R_{soil} rates were observed in the late afternoon and evening as soil temperatures were cooling back down from the daytime maxima. There was also a lag in the period of time between which maximum PAR and maximum R_{soil} were reached, and this lag was typically greater within the mesquite than the grass microhabitat (Figure 4).

[33] This observed hysteretic sensitivity of respiration to temperature (Figure 6) may be the result of abiotic or biotic drivers/processes, or some combination thereof (as discussed by *Ruehr et al.* [2010]). *Phillips et al.* [2010] note that there is currently no consensus as to the cause of this hysteresis and have shown that physical processes of heat and CO_2 transport alone could explain this pattern in some ecosystems. As has been proposed in other studies, the development of a hysteretic response may be linked to the dependence of R_{soil} on the delivery of labile carbon from recent photosynthetic activity in the canopy [*Baldocchi et al.*, 2006; *Carbone and Trumbore*, 2007; *Högberg et al.*, 2009, 2001; *Tang et al.*, 2005a]. Though concurrent measurements of diel leaf-level photosynthesis were not taken within this study period, an analysis of the relationship between R_{soil} and eddy covariance tower-based estimates of gross ecosystem production (GEP) did illustrate a significant correlation, when using the previous day's measure of GEP (data not shown). Time lags in the apparent delivery of

photosynthetic products from leaves to roots have been shown to vary on the order of hours to days for a variety of ecosystems [*Baldocchi et al.*, 2006; *Carbone and Trumbore*, 2007; *Ekblad and Högberg*, 2001; *Kuzyakov and Gavrichkova*, 2010; *Moyano et al.*, 2008; *Thompson and Holbrook*, 2003; *Vargas et al.*, 2010a], and could be relevant to both the development of the hysteresis and to the late morning depression in R_{soil} rates seen in this study. The relative contribution of autotrophic and heterotrophic respiration to total R_{soil} may vary throughout the day, as described by *Carbone et al.* [2008], with the peak autotrophic contribution occurring early in the evening after a delayed delivery of root exudates, and minimal contribution from either pool midday at peak temperatures and VPD. Similar midday drops in respiration rates have been found, predominantly in woody plants [*Carbone et al.*, 2008; *Gaumont-Guay et al.*, 2006; *Doff sotta et al.*, 2004; *Vargas and Allen*, 2008a].

[34] The hysteretic effect was most apparent within the mesquite microhabitat, and the magnitude of this effect (in terms of actual rates of R_{soil}) was greatest during the summer monsoon when the plants had the greatest canopy leaf area and were most physiologically active. The magnitude of difference between late morning and late evening rates of R_{soil} averaged 100%, with actual differences in flux rates midday versus at night for the same temperature surpassing 6 μmol CO_2 m^{-2} s^{-1}. The hysteresis effect was also found within the soils under grasses, occasionally topping 2 μmol CO_2 m^{-2} s^{-1} after rain events, though the effects were more short-lived. The greatest percent difference in flux rates at a common temperature, however, was found under mesquites in the premonsoon when midday rates approached zero, but evening rates were more than 1200% higher. Though these actual levels of flux were still small, the magnitude of error that would be generated by using a model describing respiration as a function, simple or complex, of temperature would be sizable when compounded over this 100 day season. The importance of the hysteresis effect on estimating ecosystem respiration needs to be more fully analyzed, particularly within the footprint of an EC tower where nighttime estimates of respiration often must be estimated due to insufficient turbulence to produce valid EC measurements [*Baldocchi*, 2003] and measures of net ecosystem productivity are partitioned into respiration and photosynthesis.

[35] Knowing that there is a hysteresis in this temperature response of R_{soil} informs our manual chamber R_{soil} measurement schemes and extrapolations to the ecosystem scale with those measurements, as one can no longer confidently measure R_{soil} late morning as those soil temperatures are increasing for the day and believe that the entirety of a temperature response was captured. Furthermore, the presence of this hysteretic response complicates the development of simple single-driver and multiple regression analysis to examine the relative control of multiple environmental drivers, as neither classic Arrhenius nor Q_{10} functions appropriately models efflux rates. In future analyses containing additional site years of data, not only will we use more complex CO_2 diffusion models [*Šimůnek and Suarez*, 1993] but we will also describe a suite of model-fitting techniques to examine the interactive effects of vegetative growth form, soil moisture, temperature on R_{soil}, similar to those recently been carried out by *Cable et al.* [2008] concerning soil textural properties and *Vargas et al.* [2010b] for soil CO_2 production.

5. Summary and Conclusion

[36] Inherent vegetative growth form traits influenced ecosystem-scale R_{soil} in that woody plants were physiogically active months before the native bunchgrasses, ultimately inducing to a detectable change in the landscape-level phenology of the site. R_{soil} rates under mesquites were not only greater per unit area and time, but were also elevated longer in response to isolated rain events and prolonged wetting, extending the contribution of the soils under mesquites to annual ecosystem-scale R_{soil}. The combination of increased rooting depth and the growth-form-induced reductions in evaporative demand in the soils under mesquites led to a lower degree of sensitivity of R_{soil} to soil moisture within this microhabitat. If projections of increased precipitation variability develop, this interaction between vegetative cover and climatic change may positively influence R_{soil} rates under mesquites over those under native bunchgrasses, which showed a shorter pulse duration. As woody plant encroachment in semiarid regions increases vegetative cover by mesquites, the increased GEP commonly found in these areas may be partially negated by increased ecosystem-scale R_{soil}. As such, developing an understanding of the spatiotemporal variability of the ratio GEP/R_{eco} will be important as ecosystems undergo transitions in vegetative cover.

[37] Within the mesquite microhabitat, there was a significant degree of hysteresis in the relationship between soil temperature and R_{soil} rates. In this sense, soil temperature had little direct control over R_{soil}, as rates varied by as much as 1200% and 6 μmol CO_2 m^{-2} s^{-1} for the same temperature within a 24 h period. The exact cause of this hysteretic response is not known, but like others, we hypothesize that it is linked to a lag in delivery of recently assimilated products of photosynthesis to the roots whose exudates will stimulate soil microbial respiration. Though not evidence of causation, there was a significantly positive relationship between the degree of hysteresis within the temperature response function of soil respiration under mesquite maximum rates of R_{soil} that day. If one only measured R_{soil} in the early morning, when R_{soil} fluxes were lower for a common temperature, to estimate the contribution of R_{soil} to ecosystem respiration, one would greatly underestimate this ratio. The degree of hysteresis varied significantly among vegetation types and throughout a year, suggesting that a single model parameter will not capture this dynamic variable for a mixed vegetation ecosystem. As landscape vegetative cover transitions from grasslands to shrublands, not only are the rates and durations of R_{soil} greater, but they also become more difficult to accurately estimate.

[38] At the ecosystem-scale, eddy covariance-based measures of nighttime respiration are used to estimate daytime rates of respiratory fluxes in accordance with an exponential temperature extrapolation. The results of this study highlight a potential problem in this procedure, as ecosystem-scale rates of R_{soil} were greater than total R_{eco}, which is composed of both soil and aboveground component fluxes, throughout much of the monsoon season of peak CO_2 efflux. Temporally and spatially intensive mea-

sures of mesquite and grass respiration throughout the day and night within the footprint of the tower would add great insight into this discrepancy, but to date, no relatively simple measure exists. However, such a combined approach of measured aboveground and belowground components fluxes appears necessary to validate this widely used means of estimating ecosystem-scale CO_2 efflux.

[39] **Acknowledgments.** This work was supported by Philecology Foundation of Fort Worth, Texas, and NSF-DEB 04189134 and 0414977 to T.E.H. Additional support was provided by the USDA-ARS and by SAHRA (Sustainability of semi-Arid Hydrology and Riparian Areas) under the STC Program of the National Science Foundation, agreement EAR-9876800. The authors thank J. E. Bronstein, D. L. Venable, and anonymous reviewers from *JGR-Biogeosciences* for providing insightful comments on the manuscript. We also thank A. Tyler, N. Pierce, and R. Bryant for assistance with measurements and equipment maintenance and M. McClaran and M. Heitlinger, who oversee the research carried out within the Santa Rita Experimental Range.

References

Asensio, D., J. Penuelas, J. Llusia, R. Ogaya, and L. Filella (2007), Interannual and interseasonal soil CO_2 efflux and VOC exchange rates in a Mediterranean holm oak forest in response to experimental drought, *Soil Biol. Biochem.*, *39*, 2471–2484, doi:10.1016/j.soilbio.2007.04.019.

Baldocchi, D. (2003), Assessing the eddy covariance technique for evaluating carbon dioxide exchange rates of ecosystems: Past, present and future, *Global Change Biol.*, *9*, 479–492, doi:10.1046/j.1365-2486.2003.00629.x.

Baldocchi, D., J. Tang, and L. Xu (2006), How switches and lags in biophysical regulators affect spatial-temporal variation of soil respiration in an oak-grass savanna, *J. Geophys. Res.*, *111*, G02008, doi:10.1029/2005JG000063.

Breshears, D. D., O. B. Myers, and F. J. Barnes (2009), Horizontal heterogeneity in the frequency of plant-available water with woodland intercanopy-canopy vegetation patch type rivals that occurring vertically by soil depth, *Ecohydrology.*, *2*, 503–519, doi:10.1002/eco.75.

Cable, J. M., K. Ogle, D. G. Williams, J. F. Weltzin, and T. E. Huxman (2008), Soil texture drives responses of soil respiration to precipitation pulses in the Sonoran Desert: Implications for climate change, *Ecosystems*, *11*, 961–979, doi:10.1007/s10021-008-9172-x.

Canadell, J., R. B. Jackson, J. R. Ehleringer, H. A. Mooney, O. E. Sala, and E. D. Schulze (1996), Maximum rooting depth of vegetation types at the global scale, *Oecologia*, *108*, 583–595, doi:10.1007/BF00329030.

Carbone, M. S., and S. E. Trumbore (2007), Contribution of new photosynthetic assimilates to respiration by perennial grasses and shrubs: Residence times and allocation patterns, *New Phytol.*, *176*, 124–135, doi:10.1111/j.1469-8137.2007.02153.x.

Carbone, M. S., G. C. Winston, and S. E. Trumbore (2008), Soil respiration in perennial grass and shrub ecosystems: Linking environmental controls with plant and microbial sources on seasonal and diel timescales, *J. Geophys. Res.*, *113*, G02022, doi:10.1029/2007JG000611.

Davidson, E. A., and S. E. Trumbore (1995), Gas diffusivity and production of CO_2 in deep soils of the eastern Amazon, *Tellus, Ser. B*, *47*, 550–565, doi:10.1034/j.1600-0889.47.issue5.3.x.

Davidson, E. A., E. Belk, and R. D. Boone (1998), Soil water content and temperature as independent or confounded factors controlling soil respiration in a temperate mixed hardwood forest, *Global Change Biol.*, *4*, 217–227, doi:10.1046/j.1365-2486.1998.00128.x.

Diffenbaugh, N. S., F. Giorgi, and J. S. Pal (2008), Climate change hotspots in the United States, *Geophys. Res. Lett.*, *35*, L16709, doi:10.1029/2008GL035075.

Doff sotta, E. D., P. Meir, Y. Malhi, A. D. Nobre, M. Hodnett, and J. Grace (2004), Soil CO_2 efflux in a tropical forest in the central Amazon, *Global Change Biol.*, *10*, 601–617, doi:10.1111/j.1529-8817.2003.00761.x.

Easterling, D. R., G. A. Meehl, C. Parmesan, S. A. Changnon, T. R. Karl, and L. O. Mearns (2000), Climate extremes: Observations, modeling, and impacts, *Science*, *289*, 2068–2074, doi:10.1126/science.289.5487.2068.

Ekblad, A., and P. Högberg (2001), Natural abundance of ^{13}C in CO_2 respired from forest soils reveals speed of link between tree photosynthesis and root respiration, *Oecologia*, *127*, 305–308, doi:10.1007/s004420100667.

Gaumont-Guay, D., T. A. Black, T. J. Griffis, A. G. Barr, R. S. Jassal, and Z. Nesic (2006), Interpreting the dependence of soil respiration on soil temperature and water content in a boreal aspen stand, *Agric. For. Meteorol.*, *140*, 220–235, doi:10.1016/j.agrformet.2006.08.003.

Gilmanov, T. G., et al. (2007), Partitioning European grassland net ecosystem CO_2 exchange into gross primary productivity and ecosystem respiration using light response function analysis, *Agric. Ecosyst. Environ.*, *121*, 93–120, doi:10.1016/j.agee.2006.12.008.

Glendening, G. E. (1952), Some quantitative data on the increase of mesquite and cactus on a desert grassland range in southern Arizona, *Ecology*, *33*, 319–328, doi:10.2307/1932827.

Goodale, C. L., and E. A. Davidson (2002), Carbon cycle: Uncertain sinks in the shrubs, *Nature*, *418*, 593–594, doi:10.1038/418593a.

Gordon, H. B., P. H. Whetton, A. B. Pittock, A. M. Fowler, and M. R. Haylock (1992), Simulated changes in daily precipitation intensity due to the enhanced greenhouse effect: Implications for extreme precipitation events, *Clim. Dyn.*, *8*, 83–102, doi:10.1007/BF00209165.

Goudriaan, J., and J. L. Monteith (1990), A mathematical function for crop growth based on light interception and leaf area expansion, *Ann. Bot.*, *66*, 695–701.

Groisman, P. Y. A., et al. (1999), Changes in the probability of heavy precipitation: Important indicators of climatic change, *Clim. Change*, *42*, 243–283, doi:10.1023/A:1005432803188.

Han, G. X., G. S. Zhou, Z. Z. Xu, Y. Yang, J. L. Liu, and K. Q. Shi (2007a), Biotic and abiotic factors controlling the spatial and temporal variation of soil respiration in an agricultural ecosystem, *Soil Biol. Biochem.*, *39*, 418–425, doi:10.1016/j.soilbio.2006.08.009.

Han, G. X., G. S. Zhou, Z. Z. Xu, Y. Yang, J. L. Liu, and K. Q. Shi (2007b), Soil temperature and biotic factors drive the seasonal variation of soil respiration in a maize (*Zea mays* L.) agricultural ecosystem, *Plant Soil*, *291*, 15–26, doi:10.1007/s11104-006-9170-8.

Hibbard, K. A., S. Archer, D. S. Schimel, and D. W. Valentine (2001), Biogeochemical changes accompanying woody plant encroachment in a subtropical savanna, *Ecology*, *82*, 1999–2011, doi:10.1890/0012-9658(2001)082[1999:BCAWPE]2.0.CO;2.

Hillel, D. (1993), *Introduction to Soil Physics*, Academic, San Diego, Calif.

Hirano, T., H. Kim, and Y. Tanaka (2003), Long-term half-hourly measurement of soil CO_2 concentration and soil respiration in a temperate deciduous forest, *J. Geophys. Res.*, *108*(D20), 4631, doi:10.1029/2003JD003766.

Högberg, P., A. Nordgren, N. Buchmann, A. F. S. Taylor, A. Ekblad, M. N. Högberg, G. Nyberg, M. Ohoson-Löfvenius, and D. J. Read (2001), Large-scale forest girdling shows that current photosynthesis drives soil respiration, *Nature*, *411*, 789–792, doi:10.1038/35081058.

Högberg, P., et al. (2009), High temporal resolution tracing of photosynthate carbon from the tree canopy to forest soil microorganisms, *New Phytol.*, *177*, 220–228.

Houghton, R. A., J. L. Hackler, and K. T. Lawrence (1999), The U.S. carbon budget: Contributions from land-use change, *Science*, *285*, 574–578, doi:10.1126/science.285.5427.574.

Hultine, K. R., D. F. Koepke, W. T. Pockman, A. Fravolini, J. S. Sperry, and D. G. Williams (2006), Influence of soil texture on hydraulic properties and water relations of a dominant warm-desert phreatophyte, *Tree Physiol.*, *26*, 313–323, doi:10.1093/treephys/26.3.313.

Hurtt, G. C., S. W. Pacala, P. R. Moorcroft, J. Caspersen, E. Shevliakova, R. A. Houghton, and B. Moore III (2002), Projecting the future of the U.S. carbon sink, *Proc. Natl. Acad. Sci. U. S. A.*, *99*, 1389–1394, doi:10.1073/pnas.012249999.

Irvine, J., and B. E. Law (2002), Contrasting soil respiration in young and old-growth ponderosa pine forests, *Global Change Biol.*, *8*, 1183–1194, doi:10.1046/j.1365-2486.2002.00544.x.

Ivanov, V. Y., S. Fatichi, G. D. Jenerette, J. F. Espeleta, P. A. Troch, and T. E. Huxman (2010), Hysteresis of soil moisture spatial heterogeneity and the "homogenizing" effect of vegetation, *Water Resour. Res.*, *46*, W09521, doi:10.1029/2009WR008611.

Jackson, R. B., et al. (2000), Belowground consequences of vegetation change and their treatment in models, *Ecol. Appl.*, *10*, 470–483, doi:10.1890/1051-0761(2000)010[0470:BCOVCA]2.0.CO;2.

Jenerette, G. D., and R. Lal (2005), Hydrologic sources of carbon cycling uncertainty throughout the terrestrial-aquatic continuum, *Global Change Biol.*, *11*, 1873–1882.

Jenerette, G. D., R. L. Scott, and T. E. Huxman (2008), Whole ecosystem metabolic pulses following precipitation events, *Funct. Ecol.*, *22*, 924–930, doi:10.1111/j.1365-2435.2008.01450.x.

Jury, W. A., W. R. Gardner, and W. H. Gardner (1991), *Soil Physics*, John Wiley, New York.

Kuzyakov, Y., and O. Gavrichkova (2010), Time lag between photosynthesis and carbon dioxide efflux from soil: A review of mechanisms and controls, *Global Change Biol.*, *16*, 3386–3406, doi:10.1111/j.1365-2486.2010.02179.x.

Law, B. E., F. M. Kelliher, D. D. Baldocchi, P. M. Anthoni, J. Irvine, D. Moore, and S. Van Tuyl (2001), Spatial and temporal variation in respiration in a young ponderosa pine forests during a summer drought, *Agric. For. Meteorol.*, *110*, 27–43, doi:10.1016/S0168-1923(01)00279-9.

Liang, N. S., G. Inoue, and Y. Fujinuma (2003), A multichannel automated chamber system for continuous measurement of forest soil CO_2 efflux, *Tree Physiol.*, *23*, 825–832.

Liang, N. S., T. Nakadai, T. Hirano, L. Y. Qu, T. Koike, Y. Fujinuma, and G. Inoue (2004), In situ comparison of four approaches to estimating soil CO_2 efflux in a northern larch (*Larix kaempferi* Sarg.) forest, *Agric. For. Meteorol.*, *123*, 97–117, doi:10.1016/j.agrformet.2003.10.002.

Lin, J. L., B. E. Mapes, K. M. Weickmann, G. N. Kiladis, S. D. Schubert, M. J. Suarez, J. T. Bacmeister, and M. I. Lee (2008), North American monsoon and convectively coupled equatorial waves simulated by IPCC AR4 coupled GCMs, *J. Clim.*, *21*, 2919–2937, doi:10.1175/2007JCLI1815.1.

Lloyd, J., and J. A. Taylor (1994), On the temperature-dependence of soil respiration, *Funct. Ecol.*, *8*, 315–323, doi:10.2307/2389824.

Martens, S. N., D. D. Breshears, and C. W. Meyer (2000), Spatial distributions of understory light along the grassland/forest continuum: Effects of cover, height, and spatial pattern of tree canopies, *Ecol. Modell.*, *126*, 79–93, doi:10.1016/S0304-3800(99)00188-X.

McClaran, M. P. (2003), A century of vegetation change on the Santa Rita Experimental Range, in *Santa Rita Experimental Range: 100 Years (1903–2003) of Accomplishments and Contributions*, pp. 16–33, U.S. Dep. of Agric. For. Serv., Ogden, Utah.

McCulley, R. L., S. R. Archer, T. W. Boutton, F. M. Hons, and D. A. Zuberer (2004), Soil respiration and nutrient cycling in wooded communities developing in grassland, *Ecology*, *85*, 2804–2817, doi:10.1890/03-0645.

McLain, J. E. T., and D. A. Martens (2006), Moisture controls on trace gas fluxes in semiarid riparian soils, *Soil Sci. Soc. Am. J.*, *70*, 367–377, doi:10.2136/sssaj2005.0105.

McLain, J. E. T., D. A. Martens, and M. P. McClaran (2008), Soil cycling of trace gases in response to mesquite management in a semiarid grassland, *J. Arid Environ.*, *72*, 1654–1665, doi:10.1016/j.jaridenv.2008.03.003.

McPherson, G. R. (1997), *Ecology and Management of North American Savannas*, Univ. of Ariz. Press, Tucson.

Moldrup, P., T. Olesen, T. Yamaguchi, P. Schjonning, and D. E. Rolston (1999), Modeling diffusion and reaction in soils: IX. The Buckingham-Burdine-Campbell equation for gas diffusivity in undisturbed soil, *Soil Sci.*, *164*, 542–551, doi:10.1097/00010694-199908000-00002.

Moyano, F. E., W. L. Kutsch, and C. Rebmann (2008), Soil respiration fluxes in relation to photosynthetic activity in broad-leaf and needle-leaf forest stands, *Agric. For. Meteorol.*, *148*, 135–143, doi:10.1016/j.agrformet.2007.09.006.

Myklebust, M. C., L. E. Hipps, and R. J. Ryel (2008), Comparison of eddy covariance, chamber, and gradient methods of measuring soil CO_2 efflux in an annual semi-arid grass, *Bromus tectorum*, *Agric. For. Meteorol.*, *148*, 1894–1907, doi:10.1016/j.agrformet.2008.06.016.

Pacala, S., et al. (2007), The North American carbon budget past and present, in *The First State of the Carbon Cycle Report (SOCCR): The North American Carbon Budget and Implications for the Global Carbon Cycle. A Report by the U.S. Climate Change Science Program and the Subcommittee on Global Change Research*, pp. 29–36, NOAA, Natl. Clim. Data Cent., Asheville, N. C.

Pacala, S. W., et al. (2001), Consistent land- and atmosphere-based US carbon sink estimates, *Science*, *292*, 2316–2320, doi:10.1126/science.1057320.

Parkin, T. B., and T. C. Kaspar (2003), Temperature controls on diurnal carbon dioxide flux: Implications for estimating soil carbon loss, *Soil Sci. Soc. Am. J.*, *67*, 1763–1772, doi:10.2136/sssaj2003.1763.

Phillips, C. L., N. Nickerson, D. Risk, and B. J. Bond (2010), Interpreting diel hysteresis between soil respiration and temperature, *Global Change Biol.*, *17*, 515–527, doi:10.1111/j.1365-2486.2010.02250.

Potts, D. L., T. E. Huxman, J. M. Cable, N. B. English, D. D. Ignace, J. A. Eilts, M. J. Mason, J. F. Weltzin, and D. G. Williams (2006a), Antecedent moisture and seasonal precipitation influence the response of canopy-scale carbon and water exchange to rainfall pulses in a semi-arid grassland, *New Phytol.*, *170*, 849–860, doi:10.1111/j.1469-8137.2006.01732.x.

Potts, D. L., T. E. Huxman, B. J. Enquist, J. F. Weltzin, and D. G. Williams (2006b), Resilience and resistance of ecosystem functional response to a precipitation pulse in a semi-arid grassland, *J. Ecol.*, *94*, 23–30, doi:10.1111/j.1365-2745.2005.01060.x.

Raich, J. W., and W. H. Schlesinger (1992), The global carbon-dioxide flux in soil respiration and its relationship to vegetation and climate, *Tellus, Ser. B*, *44*, 81–99, doi:10.1034/j.1600-0889.1992.t01-1-00001.x.

Reichstein, M., et al. (2005), On the separation of net ecosystem exchange into assimilation and ecosystem respiration: Review and improved algorithm, *Global Change Biol.*, *11*, 1424–1439, doi:10.1111/j.1365-2486.2005.001002.x.

Reynolds, J. F., R. A. Virginia, P. R. Kemp, A. G. de Soyza, and D. C. Tremmel (1999), Impact of drought on desert shrubs: Effects of seasonality and degree of resource island development, *Ecol. Monogr.*, *69*, 69–106, doi:10.1890/0012-9615(1999)069[0069:IODODS]2.0.CO;2.

Ricker, W. E. (1973), Linear regressions in fishery research, *J. Fish. Res. Board Can.*, *30*, 409–434.

Riveros-Iregui, D. A., R. E. Emanuel, D. J. Muth, B. L. McGlynn, H. E. Epstein, D. L. Welsch, V. J. Pacific, and J. M. Wraith (2007), Diurnal hysteresis between soil CO_2 and soil temperature is controlled by soil water content, *Geophys. Res. Lett.*, *34*, L17404, doi:10.1029/2007GL030938.

Riveros-Iregui, D. A., B. L. McGlynn, H. E. Epstein, and D. L. Welsch (2008), Interpretation and evaluation of combined measurement techniques for soil CO_2 efflux: Discrete surface chambers and continuous soil CO_2 concentration probes, *J. Geophys. Res.*, *113*, G04027, doi:10.1029/2008JG000811.

Ruehr, N. K., A. Knohl, and N. Buchmann (2010), Environmental variables controlling soil respiration on diurnal, seasonal and annual time-scales in a mixed mountain forest in Switzerland, *Biogeochemistry*, *98*, 153–170, doi:10.1007/s10533-009-9383-z.

Savage, K. E., and E. A. Davidson (2003), A comparison of manual and automated systems for soil CO_2 flux measurements: Trade-offs between spatial and temporal resolution, *J. Exp. Bot.*, *54*, 891–899, doi:10.1093/jxb/erg121.

Schenk, H. J., and R. B. Jackson (2002), Rooting depths, lateral root spreads and below-ground/above-ground allometries of plants in water-limited ecosystems, *J. Ecol.*, *90*, 480–494, doi:10.1046/j.1365-2745.2002.00682.x.

Schimel, D., et al. (2000), Contribution of increasing CO_2 and climate to carbon storage by ecosystems in the United States, *Science*, *287*, 2004–2006, doi:10.1126/science.287.5460.2004.

Schlesinger, W. H., J. F. Reynolds, G. L. Cunningham, L. F. Heunneke, W. M. Jarrel, R. A. Virginia, and W. G. Whitford (1990), Biological feedbacks in global desertification, *Science*, *247*, 1043–1048, doi:10.1126/science.247.4946.1043.

Scholes, R. J., and S. A. Archer (1997), Tree-grass interactions in savannas, *Annu. Rev. Ecol. Syst.*, *28*, 517–544, doi:10.1146/annurev.ecolsys.28.1.517.

Scott, A., I. Crichton, and B. C. Ball (1999), Long-term monitoring of soil gas fluxes with closed chambers using automated and manual systems, *J. Environ. Qual.*, *28*, 1637–1643, doi:10.2134/jeq1999.00472425002800050030x.

Scott, R. L., T. E. Huxman, D. G. Williams, and D. C. Goodrich (2006), Ecohydrological impacts of woody-plant encroachment: Seasonal patterns of water and carbon dioxide exchange within a semiarid riparian environment, *Global Change Biol.*, *12*, 311–324, doi:10.1111/j.1365-2486.2005.01093.x.

Scott, R. L., G. D. Jenerette, D. L. Potts, and T. E. Huxman (2009), Effects of seasonal drought on net carbon dioxide exchange from a woody-plant-encroached semiarid grassland, *J. Geophys. Res.*, *114*, G04004, doi:10.1029/2008JG000900.

Šimůnek, J., and D. L. Suarez (1993), Modeling of carbon dioxide transport and production in soil 1. Model development, *Water Resour. Res.*, *29*, 487–497, doi:10.1029/92WR02225.

Sponseller, R. A. (2007), Precipitation pulses and soil CO_2 flux in a Sonoran Desert ecosystem, *Global Change Biol.*, *13*, 426–436, doi:10.1111/j.1365-2486.2006.01307.x.

Stark, J. (1994), Causes of soil nutrient heterogeneity at different scales, in *Exploitation of Environmental Heterogeneity by Plants*, edited by M. M. Caldwell and R. W. Pearcy, pp. 255–284, Academic, San Diego, Calif.

Subke, J. A., I. Inglima, and M. F. Cotrufo (2006), Trends and methodological impacts in soil CO_2 efflux partitioning: A metaanalytical review, *Global Change Biol.*, *12*, 921–943, doi:10.1111/j.1365-2486.2006.01117.x.

Suwa, M., G. G. Katul, R. Oren, J. Andrews, J. Pippen, A. Mace, and W. H. Schlesinger (2004), Impact of elevated atmospheric CO_2 on forest floor respiration in a temperate pine forest, *Global Biogeochem. Cycles*, *18*, GB2013, doi:10.1029/2003GB002182.

Tang, J. W., and D. D. Baldocchi (2005), Spatial-temporal variation in soil respiration in an oak-grass savanna ecosystem in California and its partitioning into autotrophic and heterotrophic components, *Biogeochemistry*, *73*, 183–207, doi:10.1007/s10533-004-5889-6.

Tang, J. W., D. D. Baldocchi, Y. Qi, and L. K. Xu (2003), Assessing soil CO_2 efflux using continuous measurements of CO_2 profiles in soils with

small solid-state sensors, *Agric. For. Meteorol.*, *118*, 207–220, doi:10.1016/S0168-1923(03)00112-6.

Tang, J. W., D. D. Baldocchi, and L. Xu (2005a), Tree photosynthesis modulates soil respiration on a diurnal time scale, *Global Change Biol.*, *11*, 1298–1304, doi:10.1111/j.1365-2486.2005.00978.x.

Tang, J. W., L. Misson, A. Gershenson, W. X. Cheng, and A. H. Goldstein (2005b), Continuous measurements of soil respiration with and without roots in a ponderosa pine plantation in the Sierra Nevada Mountains, *Agric. For. Meteorol.*, *132*, 212–227, doi:10.1016/j.agrformet.2005.07.011.

Teuling, A. J., and P. A. Troch (2005), Improved understanding of soil moisture variability and dynamics, *Geophys. Res. Lett.*, *32*, L05404, doi:10.1029/2004GL021935.

Thompson, M. V., and N. M. Holbrook (2003), Application of a single solute non-steady-state phloem model to the study of long-distance assimilate transport, *J. Theor. Biol.*, *220*, 419–455, doi:10.1006/jtbi.2003.3115.

Throop, H. L., and S. R. Archer (2008), Shrub (*Prosopis velutina*) encroachment in a semidesert grassland: Spatial-temporal changes in soil organic carbon and nitrogen pools, *Global Change Biol.*, *14*, 2420–2431, doi:10.1111/j.1365-2486.2008.01650.x.

Treonis, A. M., D. H. Wall, and R. A. Virginia (2002), Field and microcosm studies of decomposition and soil biota in a cold desert soil, *Ecosystems*, *5*, 159–170, doi:10.1007/s10021-001-0062-8.

Turcu, V. E., S. B. Jones, and D. Or (2005), Continuous soil carbon dioxide and oxygen measurements and estimation of gradient-based gaseous flux, *Vadose Zone J.*, *4*, 1161–1169, doi:10.2136/vzj2004.0164.

Uchida, M., Y. Nojiri, N. Saigusa, and T. Oikawa (1997), Calculation of CO_2 flux from forest soil using ^{222}Rn calibrated method, *Agric. For. Meteorol.*, *87*, 301–311, doi:10.1016/S0168-1923(97)00001-4.

Van Auken, O. W. (2000), Shrub invasions of North American semiarid grasslands, *Annu. Rev. Ecol. Syst.*, *31*, 197–215, doi:10.1146/annurev.ecolsys.31.1.197.

Vargas, R., and M. F. Allen (2008a), Diel patterns of soil respiration in a tropical forest after Hurricane Wilma, *J. Geophys. Res.*, *113*, G03021, doi:10.1029/2007JG000620.

Vargas, R., and M. F. Allen (2008b), Dynamics of fine root, fungal rhizomorphs, and soil respiration in a mixed temperate forest: Integrating sensors and observations, *Vadose Zone J.*, *7*, 1055–1064, doi:10.2136/vzj2007.0138.

Vargas, R., and M. F. Allen (2008c), Environmental controls and the influence of vegetation type, fine roots and rhizomorphs on diel and seasonal variation in soil respiration, *New Phytol.*, *179*, 460–471, doi:10.1111/j.1469-8137.2008.02481.x.

Vargas, R., et al. (2010a), Looking deeper into the soil: Biophysical controls and seasonal lags of soil CO_2 production and efflux, *Ecol. Appl.*, *20*, 1569–1582, doi:10.1890/09-0693.1.

Vargas, R., M. Detto, D. D. Baldocchi, and M. F. Allen (2010b), Multiscale analysis of temporal variability of soil CO_2 production as influenced by weather and vegetation, *Global Change Biol.*, *16*, 1589–1605, doi:10.1111/j.1365-2486.2009.02111.x.

Villegas, J. C., D. D. Breshears, C. B. Zou, and D. J. Law (2010a), Ecohydrological controls of soil evaporation in deciduous drylands: How the hierarchical effects of litter, patch and vegetation mosaic cover interact with phenology and season, *J. Arid Environ.*, *74*, 595–602, doi:10.1016/j.jaridenv.2009.09.028.

Villegas, J. C., D. D. Breshears, C. B. Zou, and P. D. Royer (2010b), Seasonally pulsed heterogeneity in microclimate: Phenology and cover effects along deciduous grassland–forest continuum, *Vadose Zone J.*, *8*, 1–10.

Xu, M., and Y. Qi (2001), Soil-surface CO_2 efflux and its spatial and temporal variations in a young ponderosa pine plantation in northern California, *Global Change Biol.*, *7*, 667–677, doi:10.1046/j.1354-1013.2001.00435.x.

Zou, C. B., G. A. Barron-Gafford, and D. D. Breshears (2007), Effects of topography and woody plant canopy cover on near-ground solar radiation: Relevant energy inputs for ecohydrology and hydropedology, *Geophys. Res. Lett.*, *34*, L24S21, doi:10.1029/2007GL031484.

G. A. Barron-Gafford, B2 Earthscience, Department of Ecology and Evolutionary Biology, University of Arizona, 1041 E. Lowell St, BSW 310, Tucson, AZ 85721, USA. (gregbg@email.arizona.edu)

T. E. Huxman, Department of Ecology and Evolutionary Biology, University of Arizona, Tucson, AZ 85721, USA.

G. D. Jenerette, Department of Botany and Plant Sciences, University of California, 2150 Batchelor Hall, Riverside, CA 92521-0124, USA.

R. L. Scott, Southwest Watershed Research Center, USDA-ARS, 2000 E. Allen Rd., Tucson, AZ 85719, USA.